C. R. Geoscience 342 (2010) 453–466

Contents lists available at ScienceDirect

Comptes Rendus Geoscience

www.sciencedirect.com

Geochemistry (Geochronology)

The Late Holocene to Pleistocene tephrostratigraphic record of Lake Ohrid (Albania)

Tephrostratigraphie du Lac d'Ohrid (Albanie) pendant le Pléistocène supérieur et l'Holocène

Benoît Caron [a,*,c], Roberto Sulpizio [b], Giovanni Zanchetta [a], Giuseppe Siani [c], Roberto Santacroce [a]

[a] *Dipartimento di Scienze della Terra, via S. Maria 53, 56126 Pisa, Italy*
[b] *CIRISIVU, c/o Dipartimento Geomineralogico, via Orabona 4, 70125 Bari, Italy*
[c] *IDES-UMR 8148, Département des Sciences de la Terre, Université Paris-XI, 91405 Orsay, France*

ARTICLE INFO

Article history:
Received 26 February 2009
Accepted after revision 15 March 2010
Available online 21 May 2010

Presented by Georges Pédro

Keywords:
Tephrostratigraphy
Tephrochronology
Italian volcanoes
Lake Ohrid
Albania

Mots clés :
Téphrostratigraphie
Téphrochronologie
Volcans italiens
Lac Ohrid
Albanie

ABSTRACT

We present in this work a tephrostratigraphic record from a sediment piston core (JO 2004) from Lake Ohrid. Five tephra layers were recognised, all from explosive eruptions of southern Italy volcanoes. A multidisciplinary study was carried out, including stratigraphy, AMS ^{14}C chronology and geochemistry. The five tephra layers were correlated with terrestrial proximal counterparts and with both marine and lacustrine tephra layers already known in the central Mediterranean area. The oldest is from Pantelleria Island (P11, 131 ka BP). Other three tephra layers are from Campanian volcanoes: X6, Campanian Ignimbrite-Y5 and SMP1-Y3 (107, 39 and 31 ka BP respectively). The youngest tephra layer corresponds to the FL eruption from Etna Volcano (3.4 ka BP). In three cases these recognitions confirm previous findings in the Balkans, while two of them were for the first time recognised in the area, with a significant enlargement of the previous assessed dispersal areas.

RÉSUMÉ

Une étude téphrostratigraphique a été réalisée dans la carotte sédimentaire JO 2004 prélevée dans le Lac d'Ohrid. Cette étude bénéficie d'un cadre chronologique établi par sept datations SMA ^{14}C et par des analyses chimiques des éléments majeurs. Cinq niveaux de tephra ont été détectés et corrélés aux dépôts terrestres proximaux ainsi qu'aux tephra identifiés dans des carottes marines et lacustres de la Méditerranée centrale. Leur origine a été attribuée au volcanisme explosif du Sud de l'Italie et corrélée à l'activité de l'Île de Pantelleria (P11, 131 ka BP), à la région campanienne (X6, 107 ka ; Ignimbrite campanienne-Y5, 39 ka ; SMP1-Y3 ; 31 ka) et à l'éruption FL de l'Etna (3,4 ka BP). Ces résultats sont en accord avec des travaux précédemment publiés dans la région des Balkans et ont permis d'identifier pour la première fois deux tephra (X6 et P11), en élargissant significativement leurs secteurs de dispersion en Méditerranéenne centrale.

* Corresponding author.
E-mail address: caron@dst.unipi.it (B. Caron).

1631-0713/$ – see front matter
doi:10.1016/j.crte.2010.03.007

1. Introduction

Tephrostratigraphy is a powerful tool that is widely applied to volcanology, Quaternary Science, palaeoceanography or archaeology. This is particularly true in the central Mediterranean region, which has borne witness to frequent and powerful volcanic explosive activity during both Holocene and Late Pleistocene (Coltelli et al., 2000; De Vivo et al., 2001; Di Vito et al., 2008; Keller et al., 1978; Mahood and Hildreth, 1986; Pappalardo et al., 1999; Paterne et al., 1988; Paterne et al., 1990; Poli et al., 1987; Santacroce, 1987; Santacroce et al., 2008; Siani et al., 2004; Sulpizio et al., 2003; Vezzoli, 1988; Wulf et al., 2004). Some of the tephra layers generated during these explosive eruptions have regional or extra-regional relevance (e.g. Y3, Y5, Y6, Y7, X5 and X6 tephra layers) (Giacco et al., 2008; Keller et al., 1978; Margari et al., 2007; Pyle et al., 2006; Sulpizio et al., 2003; Thunnell et al., 1978; Zanchetta et al., 2008), since they covered very wide areas, facilitating correlations between different geological archives. Many other tephra layers are less dispersed, but are frequently recognised in marine and lacustrine cores drilled in the central Mediterranean area (Calanchi et al., 1998; Lowe et al., 2007; Macdonald, 1974; Magny et al., 2006; Magny et al., 2007; Paterne et al., 1988; Paterne et al., 2008; Sulpizio et al., 2008; Wagner et al., 2008b; Wulf et al., 2004).

Owing to its position downwind of the Italian volcanoes, the Balkans were affected by tephra deposition during Holocene and Late Pleistocene (Sulpizio et al., 2010; Wagner et al., 2008b) (Fig. 1), but tephrostratigraphic studies are few. This article deals with the study of a long core (JO 2004; 9.88 m of length), collected on the Albanian side of Lake Ohrid, which records the last 130–140 ka of

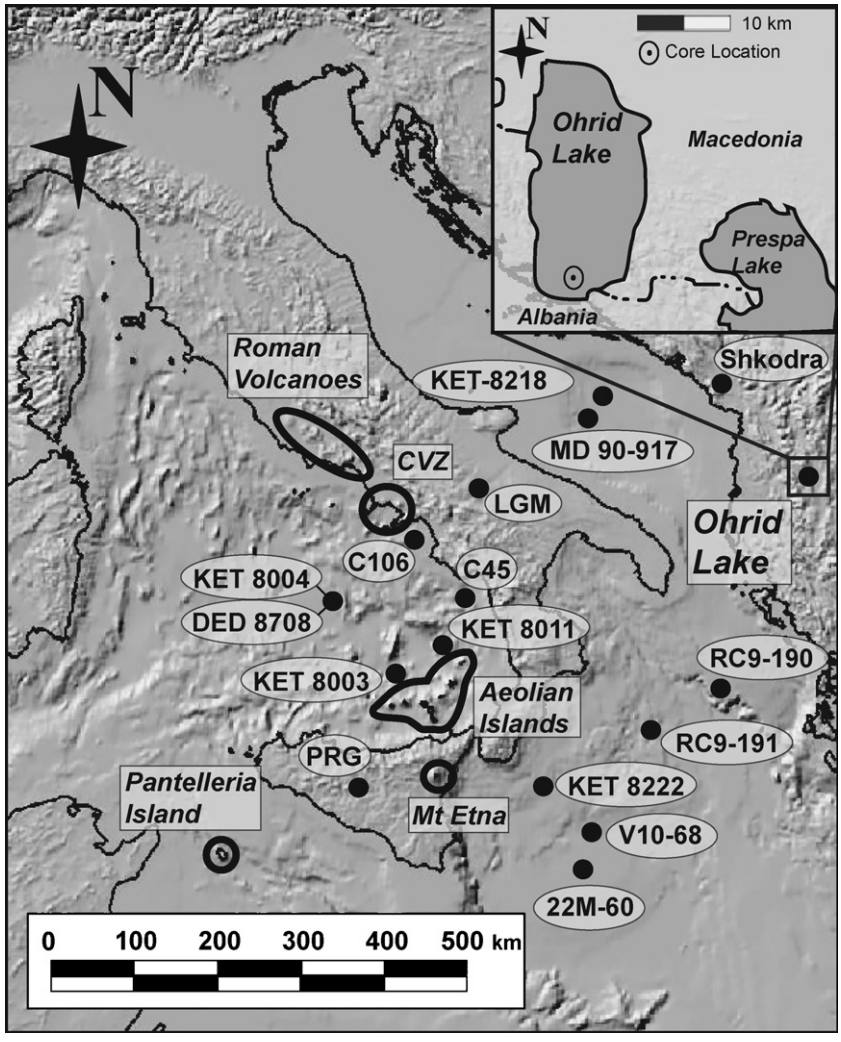

Fig. 1. Location map of the study area. The Italian volcanoes active in the investigated time span and the location of cores used in this study are shown: CVZ: Campanian Volcanic Zone (Campi Flegrei, Somma-Vesuvius, Ischia and Procida volcanoes); PRG: Lake of Pergusa; LGM: Lago Grande di Monticchio. The insert in the upper right corner reports the location of the core JO 2004.

Fig. 1. Carte de localisation du site d'étude. Les principaux volcans italiens actifs lors de la période étudiée et les sites des carottes utilisées dans cet article sont indiqués : CVZ : Campanian Volcanic Zone (Champs Phlégréens, Somma-Vesuvius, Ischia et Procida) ; PRG : lac de Pergusa ; LGM : Lago Grande di Monticchio. En haut à droite, la position du site de forage de la carotte JO 2004.

sedimentation (Lézine et al., 2010). Our aim is to provide a tephrostratigraphic reconstruction of the core JO 2004, and to provide the correlation of its tephra layers with marine, lacustrine or terrestrial deposits in the central Mediterranean. The correlation among the different archives provides an updated framework of the tephra dispersion in the central Mediterranean area, and, particularly, in the Balkans.

Few tephra studies have been carried out in the Balkans (Sulpizio et al., 2010; Wagner et al., 2008b), although their downwind position from the Italian volcanoes makes the area particularly subjected to distal ash deposition. On the other hand, the recognition of ash layers from Italian volcanoes in the Balkans contributes to shedding light into the complex and poorly understood dynamics of dispersal of ash particles during and after explosive eruptions.

2. Site description

The Ohrid Lake is one of the oldest lakes in Europe (Stankovic, 1960), and is located at the border between Albania and Macedonia (40°54′- 41°10′ N; 20°38′- 20°48′ E) (Fig. 1). The lake is at 705 m a.s.l., and has a surface of about 360 km^2. Bathymetric measurements revealed that the lake has simple, tub-shaped basin morphology with a maximum water depth of 289 m (Stankovic, 1960). It is surrounded by two principals mountain chains: the Galiçica Mountains to the east (more than 1750 m a.s.l.), and the Mokra Mountains to the west (around 1500 m a.s.l.). The Lake Ohrid has a north-south orientation, and is located in a graben, which formed during the extension of the Albanian area during the Pleistocene (Aliaj et al., 2001; Wagner et al., 2008b). The Ohrid–Korca seismic zone comprises the Pliocene–Quaternary normal-fault-controlled Ohrid graben, and the Korca and Erseka half grabens, which are generally north trending (Aliaj, 2000; Aliaj et al., 2004). Active normal faulting with horst and graben structures is seen in the geomorphology and also determined from earthquake focal mechanisms (Aliaj et al., 2001; Goldsworthy et al., 2002).

Carbonate rocks of Triassic and Jurassic age crop out to the north and to the east, while ophiolitic rocks of Jurassic age crop out to the southwest. The southern end of the basin connects with a small graben filled by continental mudstones and sandstones of Pliocene age, overlain by fluvio-lacustrine sediments of Holocene age (Nicot and Chardon, 1983). Today, roughly half of its water is derived from a number of springs located in the southeast part of the lake, draining a karstic system fed by water from the nearby Lake Prespa (20 km to the southeast and 150 m higher than Lake Ohrid), and infiltration of rainwater (700 mm/yr on average) from the Galiçica mountain range. The remaining water comes from rivers (e.g. the Sateska River to the north) and from direct meteoric precipitation. The Black Drin River is the only surface outflow to the north part of the Lake Ohrid (Anovski et al., 1980; Lézine et al., 2010; Matzinger et al., 2006; Stankovic, 1960). Lakes with comparable volume and water depth, located in temperate and Mediterranean regions, are, in general, monomictic, with a mixing of the water column during winter (Wagner et al., 2008a). Complete overturn of the water column in Lake Ohrid occurs very irregularly, roughly every 7 years (Hadzisce, 1966; Stankovic and Hadzisce, 1953). Recent investigations have shown that in years without complete overturn the water column is mixed down to depths of 125–175 m during winter (Matzinger et al., 2006).

3. Materials and methods

Two series of piston cores (JO 2004-1 and JO 2004-1a) were drilled in the southwestern part of the Lake Orhid (Lézine et al., 2010) (40° 55,000′ N ; 20° 40,297′ E; WGS 84 reference ; Fig. 1), in a water depth of 100 m. The uppermost roughly 10 m of sediments were recovered using a cable-operated piston-core (63 mm in diameter and 3 m-long; Niederreiter Corer). In order to obtain a continuous sediment record, four sections were cored from a first drilling site (labelled JO 2004-1; Fig. 2), and three sections with a planed depth offset of 1.5 m from a second drilling site located at about 5 m of distance from the first (labelled JO 2004-1a; Fig. 2). The overlapping sections were correlated using marker layers clearly identified in both cores and the resulting composite profile checked for consistency using the magnetic susceptibility record (Fig. 2b).

The magnetic susceptibility of core JO 2004 has not permitted the identification of any tephra layer, due to the high noise induced by the magnetic minerals from the drainage basin bedrocks (Wagner et al., 2008b). Tephra layer were identified by both visual inspection and continuously sampling the composite profile at 1 cm-interval, and washing and sieving each sample at 125, 63 and 40 μm using distilled water. The different grain-size fractions were dried in a laboratory heater at a temperature of 50 °C over 24 h. The three sediment fractions were carefully inspected under a stereomicroscope, looking for volcanic particles (i.e. glass shards, pumice, magmatic crystals, volcanic lithics). At least 400 particles were counted under the stereo-microscope to obtain the glass abundance.

In samples with volcanic glass in excess of 10%, glass shards and micropumice fragments were picked and sealed in resin beads. They were then polished to avoid compositional variations caused by surface alteration processes.

Major element compositions of the glass were obtained using an EDAX-DX micro-analyser (EDS analyses) mounted on a Philips SEM 515 at Dipartimento di Scienze della Terra (University of Pisa). Operating conditions were: 20 kV acceleration voltage, 100 s live counting, 10^{-9} Å beam current, beam diameter ≈500 μm, 2100 shots per second, with ZAF correction (Z: atomic number; A: absorption; and F: fluorescence). The ZAF correction procedure does not include natural or synthetic standards for reference, and requires the analyses normalization at a given value (which is chosen at 100%). Instrument calibration and performance are described in Marianelli and Sbrana (1998).

The composition of glass was classified using the Total Alkali vs. Silica diagram (TAS, Le Bas et al. (1986), Fig. 3a). Major element compositions allowed the discrimination

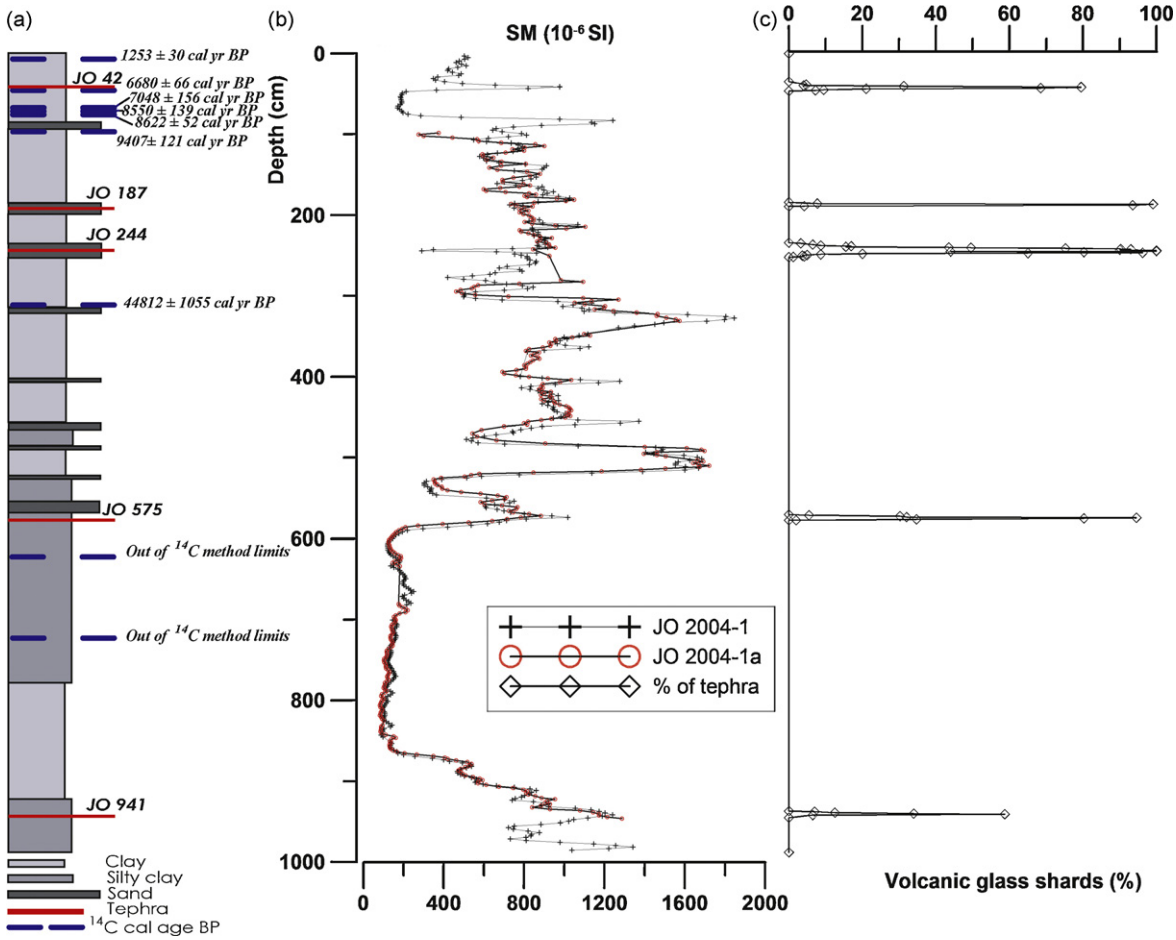

Fig. 2. Composite stratigraphy of the core JO 2004 (depth in cm): (a) lithostratigraphy (modified from Lézine et al., 2010) with tephra layers and calibrated ^{14}C ages; (b) magnetic susceptibility curve; (c) relative glass shards abundance.

Fig. 2. Stratigraphie recomposée de la carotte JO 2004 (profondeur en centimètre) : (a) lithostratigraphie (modifiée à partir de Lézine et al., 2010) avec les niveaux de tephra et les âges ^{14}C calibrés ; (b) courbe de susceptibilité magnétique ; (c) abondance relative des esquilles de verres volcaniques.

among different volcanic sources and correlation to proximal deposits of known explosive eruptions (Santacroce et al., 2008; Wulf et al., 2004).

Seven ^{14}C datings were available from literature (Lézine et al., 2010) (Table 1; Fig. 2a). Raw radiocarbon measurements were converted into calibrated ages using the INTCAL04 method (Reimer et al., 2004) and the polynomial equation of Bard et al. (1998) for ^{14}C ages older than 26 cal ka BP.

4. Results

Five tephra layers were recognised along the composite profile, and labelled JO-941 (938–942 cm), JO-575 (571–577 cm), JO-244 (235–252 cm), JO-187 (185.5–188.5 cm) and JO-42 (36.5–45.5 cm), respectively (Fig. 2a and b).

4.1. Cryptotephra JO-941 (938–942 cm)

The deepest tephra is dispersed in the sediment (cryptotephra), and glass shards were recognised in all the three sieving classes. The peak of abundance of glass particles is at 941 cm (60%; Fig. 2c), and comprises transparent, brown-honey, cuspated, thin glass shards (Fig. 4a). The groundmass is glassy, and EDS analyses show a homogeneous rhyolitic composition (Fig. 3a and b, Table 2). In the diagram Comendite-Pantellerite (FeO vs. Al_2O_3; (Macdonald, 1974)), all the analysed samples plot into the pantelleritic field.

4.2. Cryptotephra JO-575 (571–577 cm)

This cryptotephra mainly comprises white to light-brown, elongated and cuspated glass shards and rare, white micropumice fragments (Fig. 4b). The peak abundance of glass shards is between 574 and 575 cm (95%; Fig. 2c). The groundmass is glassy (Fig. 4b), and the composition shows a small variability within the trachyphonolitic field (Fig. 3a and c; Table 2).

4.3. Tephra layer JO-244 (235–252 cm)

This tephra layer is composed of two distinct parts with different colours. The first one (between 244 and 244.5 cm)

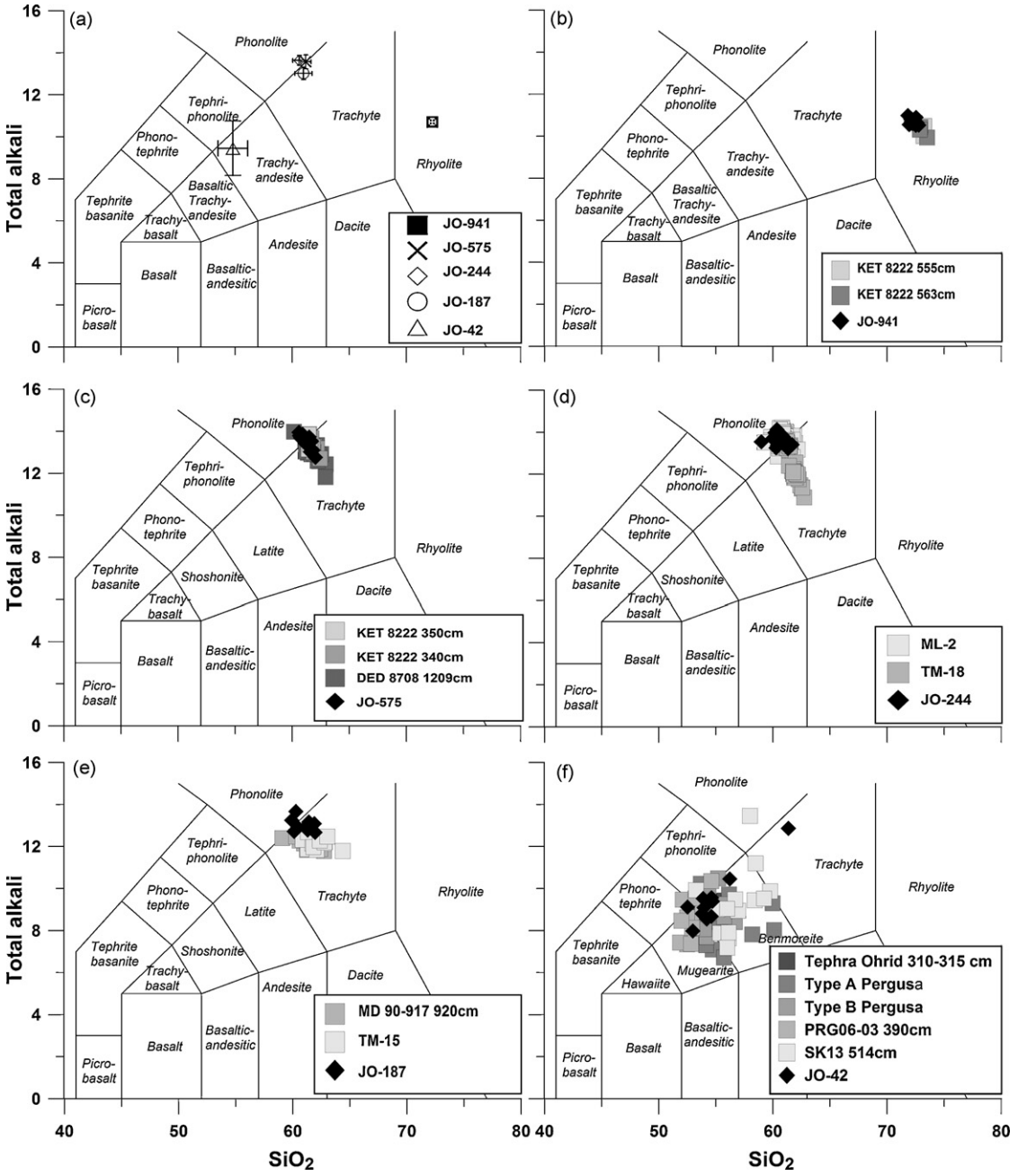

Fig. 3. Chemical classification of the studied tephra layers and comparison with tephra from literature using the Total Alkali vs. Silica (TAS) diagram (Le Bas et al., 1986): (a) general classification using average glass analyses of the five identified tephra layers (1σ error bars are also reported); (b) analyses of JO-941 cryptotephra and KET 8222-563 and 555 cm tephra (Paterne et al., 2008); (c) analyses of JO-575 cryptotephra and KET 8222-350, 340 cm and DED 8708–1209 cm tephra (Paterne, 1985; Paterne et al., 2008); (d) analyses of JO-244 tephra layer. Compositions of TM-18 (Wulf et al., 2004) and ML-2 (Margari et al., 2007) tephra layers are reported for comparison; (e) analyses of JO-187 tephra layer. Compositions of TM-15 (Wulf et al., 2004) and MD90-917 920 cm (Zanchetta et al., 2008) tephra layers are reported for comparison; (f) analyses of JO-42 cryptotephra. Compositions of SK13 514 cm (Sadori and Narcisi, 2001), PRG06-03 390 cm (Sulpizio et al., 2010), Ohrid 310–315 cm (Wagner et al., 2008b), and Pergusa Type A and B (Sadori and Narcisi, 2001) tephra layers are reported for comparison.

Fig. 3. Comparaison entre les compositions chimiques des niveaux de tephra identifiés et ceux issus de la littérature dans un diagramme Total Alcalin vs. Silice (TAS) (Le Bas et al., 1986) : (a) diagramme général des moyennes des analyses sur les verres des cinq niveaux de tephra (barre d'erreur 1σ) ; (b) analyses du crytotephra JO-941 comparées aux niveaux de tephra KET 8222-563 et 555 cm d'après Paterne et al. (2008) ; (c) analyses du crytotephra JO-575 comparées aux niveaux de tephra KET 8222-350, 340 cm et DED 8708–1209 cm d'après Paterne (1985) et Paterne et al. (2008) ; (d) analyses du niveau de tephra JO-244 comparées aux niveaux de tephra TM-18 d'après Wulf et al. (2004) et ML-2 d'après Margari et al. (2007) ; (e) analyses du niveau de tephra JO-187 comparées aux niveaux de tephra TM-15 d'après Wulf et al. (2004) et MD 90-917 d'après Zanchetta et al. (2008) ; (f) analyses du crytotephra JO-42 comparées aux niveaux de tephra de SK13 514 cm d'après Sadori et Narcisi (2001) et PRG06-03 390 cm d'après Sulpizio et al. (2010), Ohrid 310–315 cm d'après Wagner et al. (2008b) et Pergusa Type A et B d'après Sadori et Narcisi (2001).

Table 1
^{14}C ages from JO 2004 core determined at UMS-ARTEMIS (Pelletron 3MV) AMS facilities (CNRS-CEA Saclay, France (Lézine et al., 2010)). Ages were calibrated using INT CAL04 (Reimer et al., 2004) for ^{14}C age younger than 26 cal ka BP and Bard polynomial equation for age older than 26 cal ka BP (Bard et al., 1998).

Tableau 1
Tableau des âges AMS ^{14}C de la carotte JO 2004 obtenus par UMS-ARTEMIS (Pelletron 3MV) CNRS-CEA Saclay, France (Lézine et al., 2010). Les âges ont été calibrés avec INT CAL04 (Reimer et al., 2004) pour les datations d'âge inférieur à 26 cal ka BP et avec le polynôme de Bard pour les datations d'âge supérieur à 26 cal ka (Bard et al., 1998).

Laboratory number (Artemis-Saclay)	Sample	Mean composite depth (cm)	^{14}C age	Error	Age cal final	Error 1 s	Methods
SacA 8010	JO2004-1A020	20.5	1285	30	1253	30	intcal04 (Reimer et al., 2004)
SacA 8011	JO2004-1A059	59.5	5840	35	6680	66	intcal04 (Reimer et al., 2004)
2653	JO2004-1A074	74	6130	80	7048	156	intcal04 (Reimer et al., 2004)
2654	JO2004-1A078	78.5	7800	80	8550	139	intcal04 (Reimer et al., 2004)
SacA 8012	JO2004-1A085	85.5	7850	40	8622	52	intcal04 (Reimer et al., 2004)
SacA 8013	JO2004-1A100	100.5	8275	40	9407	121	intcal04 (Reimer et al., 2004)
2655	JO2004-1B113	307.6	39,100	1200	44,812	1055	Bard et al. (1998)

is yellowish gray (5Y 7/2; (GSA, 1991)), while the second one (between 247 and 248 cm) is moderate olive brown (5Y 4/4; (GSA, 1991)). The tephra comprises white, vesicular micropumices and elongated glass shards with thin septa. Most of the glass shards are transparent, with few dark-brown in colour (Fig. 4c). The abundance of glass shards and micropumice has its maximum (100%) between 244 and 244.5 cm (Fig. 2c). The groundmass is glassy (Fig. 4c), and the glass composition is trachy-phonolitic (Fig. 3a and d; Table 2).

4.4. Tephra layer JO-187 (185.5–188.5 cm)

This tephra layer is yellowish gray in colour (5Y 4/1; (GSA, 1991)), and comprises transparent, tubular, elongated micropumice fragments and transparent, brownish glass shards (Fig. 4d). The maximum abundance (99%) is at 187 cm (Fig. 2c). The groundmass is glassy (Fig. 4d), and the glass composition is homogeneous and trachytic (Fig. 3a and e; Table 2).

4.5. Cryptotephra JO-42 (36.5–45.5 cm)

This cryptotephra has a peak abundance of glass particles (80%) at 42 cm of depth (Fig. 2c), and comprises dark-brown, blocky, tachylitic fragments with few spherical vesicles (Fig. 4e). The groundmass comprises small crystals of plagioclase, clinopyroxene and minor olivine (Fig. 4e). The glass composition ranges between mugearites and benmoreites (Fig. 3a and f).

5. Discussion

5.1. Correlation of tephra layers

The K- to Na-alkaline affinity of glass compositions of the five tephra layers recognised in the core JO 2004 indicate that all of them were from explosive eruptions of Italian volcanoes, since during Late Quaternary the products of the Aegean arc were characterised by calc-alkaline affinity (Keller et al., 1978; Paterne et al., 2008; Thunnell et al., 1978). Two of them (JO-941 and JO-42) present peculiar glass compositions that indicate a source from Pantelleria Island and from Mount Etna, respectively. The other three tephras display trachytic to phonolitic composition, and can be correlated to the explosive activity of Campanian volcanoes. In the following, the precise correlation of each tephra layer with a specific eruption of these volcanoes will be discussed in detail. For comparison, the average compositions of the correlated tephra layers are reported in Table 3.

5.1.1. Cryptotephra JO-941

The pantelleritic glass composition of cryptotephra JO-941 (Table 2) indicates it was generated from Pantelleria Island. The Island of Pantelleria produced several large explosive eruptions with pantelleritic composition (Mahood and Hildreth, 1986). Among them, the most dispersed are the Green Tuff (45–50 ka), the Ignimbrite Q (113.9 ± 3.6 ka), the Ignimbrite P (133.1 ± 3.3 ka), the Welded tuff S (162–164 ka) and the Welded tuff M (174.8 ± 2.8 ka; (Mahood and Hildreth, 1986)). Two other ^{40}Ar/^{39}Ar datings are available for the Ignimbrite P (126.8 ± 1.5 ka; (La Felice et al., 2009)) and for the Welded tuff S (174.5 ± 1.5 ka; (La Felice et al., 2009)). Pantelleritic tephra layers have been found in the Ionian Sea core KET 8222 (Paterne et al., 2008) (Table 3) and named P11 (estimated age at about 131 ka, 555 cm depth) and P12 (estimated age at about 164 ka, 765 cm depth), which have similar ages as Ignimbrite P and Welded tuff S. The composition of P11 and P12 is quite similar, and the two tephra layers are hardly distinguishable on the basis of major elements.

The glass composition of sample JO-941 matches well that of both tephra layers P11 and P12 (Tables 2 and 3, Fig. 3b). Indeed, the tephra layer P11 has been recognised over a wide area of the Ionian Sea while the dispersal of P12 is more limited (Paterne et al., 2008). Nevertheless, stratigraphic and paleoclimatic considerations support the correlation of the JO-941 cm tephra with P11 marine tephra layer, and then with Ignimbrite P deposits on Pantelleria Island. This is because both carbonate and pollen curves carried out on JO 2004 core sediments (Lézine et al., 2010) unequivocally indicate that these tephra were emplaced close to the inception of the Last Interglacial. The onset of the Last Interglacial may have been recorded at different times in different archives

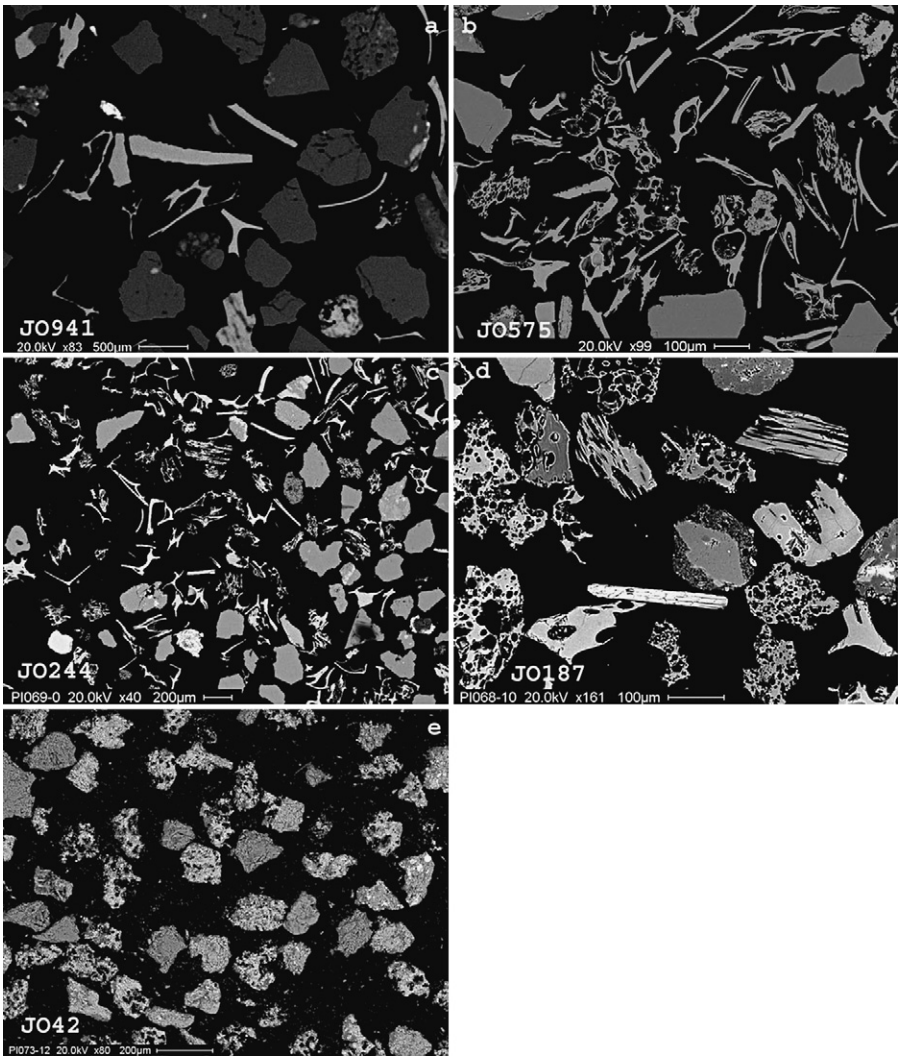

Fig. 4. Scanning Electron Microscope (SEM) pictures of volcanic particles from the five studied tephra layers and cryptotephra: (a) JO-941. Note the elongated glass shards with glassy groundmass; (b) JO-575. Note the coexistence of elongated glass shards and vesicular micropumices, both with glassy groundmass; (c) JO-244. Note the coexistence of elongated glass shards with thin septa and vesicular micropumices, both groundmass are glassy; (d) JO-187. Note the coexistence of convoluted glass shards and vesicular micropumice, both with glassy groundmass; (e) JO-42. Note the blocky shape of the tachylitic fragments, which contain few spherical vesicles. The groundmass comprises small crystals of plagioclase, clinopyroxene and olivine.

Fig. 4. Images au microscope électronique à balayage (MEB) des tephra volcaniques des niveaux (a) JO-941 composé d'esquilles de verre fines et allongées dont la matrice est vitreuse ; (b) JO-575 composé d'esquilles de verre allongées ainsi que microponces vésiculées, dont chacune des matrices est vitreuse ; (c) JO-244 composé d'esquilles de verre allongées avec de fines parois et de microponces vésiculées, dont chacune des matrices est vitreuse ; (d) JO-187 composé d'esquille de verre et de microponces allongées et fibreuses, dont chacune des matrices est vitreuse ; (e) JO-42 composé de fragments de blocs et de tachylites finement vésiculées dont la matrice se compose de petits cristaux de plagioclase, de clinopyroxènes et d'olivine.

(Tzedakis et al., 2003), but, in any case, the age of 164 ka (which corresponds to P12 tephra layer) is too old of some 10,000 years with respect to that commonly accepted for the inception of Last Interglacial at Mediterranean latitudes (e.g. 126.8 and 120.3 ka; (Tzedakis et al., 2003)).

The recognition of tephra layer P11 is the first in the Balkans, and significantly enlarges its dispersal well beyond the Ionian Sea (Fig. 5a).

5.1.2. Cryptotephra JO-575

This low alkali ratio (LAR) trachytic tephra layer occurs between the calibrated ^{14}C age of 44,812 ± 1055 cal yr BP (Lézine et al., 2010) (Table 1) and the P11 tephra layer.

Composition of the tephra layer JO-575 shows a good match with marine tephra C-31 (KET 8222 and DED 8708 deep-sea cores, Fig. 3c and Table 3), which has an interpolated age of 107 ka (Paterne et al., 2008). Paterne had related the C-31 tephra with the LAR-trachyte X6 from the 22M-60 core (Keller et al., 1978). This supports the correlation of JO-575 sample to the X6 tephra layer. The age of X6 tephra layer at 107 ka is also supported by extrapolation of the X5 tephra layer age (105 ± 2 ka; $^{40}Ar/^{39}Ar$ technique) (Kraml, 1997) based on sedimentation rate extrapolation. The source of the X6 eruption has been located in the Campanian volcanic zone (Keller et al., 1978). The X6 tephra layer was for the first time described in Ionian

Table 2
Composition of major elements of the five tephra layers recognised in core JO 2004.

Tableau 2
Compositions des éléments majeurs des cinq niveaux de tephra identifiés dans la carotte JO 2004.

JO941	SiO_2	TiO_2	Al_2O_3	FeO_{tot}	MnO	MgO	CaO	Na_2O	K_2O	P_2O_5	ClO	Total	Total Alkali
JO941-1	71.81	0.50	8.37	6.89	0.37	0.00	0.32	6.63	4.36	0.00	0.76	100.01	10.99
JO941-2	72.30	0.44	8.55	6.79	0.25	0.11	0.19	6.35	4.43	0.00	0.61	100.02	10.78
JO941-3	72.13	0.51	8.34	6.83	0.39	0.00	0.29	6.49	4.34	0.00	0.68	100.00	10.83
JO941-4	72.52	0.32	8.63	6.69	0.24	0.80	0.34	5.93	4.59	0.00	0.66	100.72	10.52
JO941-5	72.53	0.23	8.54	6.67	0.16	0.00	0.23	6.53	4.37	0.00	0.75	100.01	10.90
JO941-6	71.93	0.45	8.49	6.97	0.49	0.12	0.31	6.30	4.25	0.00	0.69	100.00	10.55
JO941-7	72.77	0.29	8.60	6.72	0.20	0.00	0.21	6.16	4.37	0.00	0.67	99.99	10.53
JO941-8	72.30	0.35	8.62	6.83	0.23	0.08	0.22	6.41	4.29	0.00	0.67	100.00	10.70
JO941-9	72.07	0.27	8.61	6.91	0.23	0.10	0.32	6.44	4.37	0.00	0.68	100.00	10.81
JO941-10	72.24	0.32	8.53	6.85	0.38	0.00	0.32	6.18	4.42	0.00	0.76	100.00	10.60
JO941-11	72.30	0.45	8.54	6.64	0.26	0.10	0.36	6.21	4.50	0.00	0.64	100.00	10.71
JO941-12	72.61	0.17	8.68	6.63	0.18	0.00	0.34	6.33	4.32	0.00	0.74	100.00	10.65
JO941-13	72.11	0.49	8.57	6.81	0.34	0.04	0.26	6.28	4.42	0.00	0.68	100.00	10.70
Mean	**72.28**	**0.37**	**8.54**	**6.79**	**0.29**	**0.10**	**0.29**	**6.33**	**4.39**	**0.00**	**0.69**	–	**10.71**
Sd	*0.28*	*0.11*	*0.10*	*0.11*	*0.10*	*0.21*	*0.06*	*0.18*	*0.09*	*0.00*	*0.05*	–	–
JO575	SiO_2	TiO_2	Al_2O_3	FeO_{tot}	MnO	MgO	CaO	Na_2O	K_2O	P_2O_5	ClO	Total	Total Alkali
JO575-1	60.59	0.53	18.42	3.24	0.39	0.27	1.78	7.29	6.66	0	0.82	99.99	13.95
JO575-2	61.01	0.59	18.86	2.85	0.31	0.38	1.54	6.82	6.93	0	0.71	100	13.75
JO575-3	60.9	0.44	18.46	3.13	0.2	0.31	1.84	7.08	6.76	0	0.87	99.99	13.84
JO575-4	60.9	0.46	18.84	2.93	0.21	0.26	1.68	7.28	6.57	0	0.88	100.01	13.85
JO575-5	60.71	0.5	18.63	3.08	0.4	0.47	1.63	6.85	6.94	0	0.78	99.99	13.79
JO575-6	61.69	0.5	18.53	2.78	0.23	0.46	1.69	5.8	7.74	0	0.57	99.99	13.54
JO575-7	61.48	0.36	18.74	2.8	0.13	0.36	1.84	5.62	8.11	0	0.57	100.01	13.73
JO575-8	61.16	0.46	18.69	3	0.3	0.3	1.65	6.86	6.85	0	0.73	100	13.71
JO575-9	60.69	0.61	18.54	3.21	0.4	0.39	1.59	7.2	6.56	0	0.81	100	13.76
JO575-10	61.67	0.43	18.64	2.93	0.3	0.5	1.59	6.02	7.49	0	0.44	100.01	13.51
JO575-11	61.68	0.64	18.79	2.82	0.42	0.35	1.5	6.33	6.81	0	0.65	99.99	13.14
JO575-12	61.13	0.5	18.9	3.1	0.38	0.3	1.51	6.7	6.73	0	0.75	100	13.43
JO575-13	61.83	0.52	18.69	2.95	0.27	0.43	1.56	5.56	7.54	0	0.64	99.99	13.1
JO575-14	61.58	0.49	19.07	2.69	0.28	0.52	1.76	5.53	7.49	0	0.59	100	13.02
JO575-15	61.11	0.37	18.85	3	0.24	0.43	1.59	6.73	6.87	0	0.8	99.99	13.6
JO575-16	60.65	0.46	18.74	3.13	0.36	0.3	1.7	7.22	6.58	0	0.85	99.99	13.8
JO575-17	60.73	0.35	18.92	3.02	0.34	0.35	1.73	7.08	6.6	0	0.88	100	13.68
JO575-18	61.43	0.36	18.66	2.87	0.2	0.46	1.74	6	7.7	0	0.57	99.99	13.7
JO575-19	62.04	0.38	18.96	2.86	0.24	0.42	1.61	5.87	6.89	0	0.73	100	12.76
JO575-20	60.92	0.41	18.87	3.09	0.2	0.38	1.45	6.96	6.89	0	0.82	99.99	13.85
Mean	**61.2**	**0.47**	**18.74**	**2.97**	**0.29**	**0.38**	**1.65**	**6.54**	**7.04**	**0**	**0.72**	–	**13.58**
Sd	*0.45*	*0.08*	*0.17*	*0.15*	*0.08*	*0.08*	*0.11*	*0.63*	*0.46*	*0*	*0.13*	–	–
JO244	SiO_2	TiO_2	Al_2O_3	FeO_{tot}	MnO	MgO	CaO	Na_2O	K_2O	P_2O_5	ClO	Total	Total Alkali
JO244-1	60.87	0.46	19.19	2.97	0.2	0.38	1.59	6.62	7.08	0	0.65	100.01	13.7
JO244-2	61.16	0.33	19.08	2.93	0.2	0.34	1.81	5.98	7.49	0	0.68	100	13.47
JO244-3	60.68	0.42	19.04	2.94	0.21	0.38	1.88	6.25	7.51	0	0.68	99.99	13.76
JO244-4	60.6	0.52	19.17	2.85	0.25	0.35	1.69	6.53	7.24	0	0.8	100	13.77
JO244-5	60.57	0.51	19.11	2.9	0.31	0.51	1.68	6.58	7.17	0	0.65	99.99	13.75
JO244-6	59.96	0.36	19.47	3.14	0.23	0.4	1.92	6.1	7.6	0	0.82	100	13.7
JO244-7	61	0.38	19.1	2.86	0.18	0.28	1.78	6.48	7.22	0	0.71	99.99	13.7
JO244-8	60.62	0.55	19.09	2.99	0.26	0.47	1.75	6.37	7.31	0	0.61	100.02	13.68
JO244-9	60.34	0.37	19.84	2.97	0.2	0.4	1.73	6.21	7.28	0	0.66	100	13.49
JO244-10	61.67	0.44	19.08	2.65	0.15	0.36	1.68	6.07	7.34	0	0.58	100.02	13.41
JO244-11	58.97	0.45	19.68	3.48	0.07	0.8	2.6	5.08	8.46	0	0.41	100	13.54
JO244-12	60.93	0.36	19	2.99	0.21	0.22	1.73	6.42	7.35	0	0.79	100	13.77
JO244-13	60.86	0.45	19.08	2.87	0.21	0.32	1.7	6.37	7.39	0	0.75	100	13.76
JO244-14	60.78	0.45	18.97	2.93	0.19	0.42	1.8	6.33	7.39	0	0.75	100.01	13.72
JO244-15	61.31	0.26	19.25	2.92	0.19	0.34	1.8	5.65	7.57	0	0.71	100	13.22
JO244-16	60.16	0.49	19.13	2.98	0.28	0.42	1.87	6.13	7.84	0	0.71	100.01	13.97
JO244-18	60.76	0.29	18.94	2.96	0.28	0.37	1.83	6.39	7.49	0	0.7	100.01	13.88
JO244-19	60.35	0.46	18.97	2.97	0.2	0.4	1.72	6.31	7.82	0	0.81	100.01	14.13
Mean	**60.64**	**0.42**	**19.18**	**2.96**	**0.21**	**0.4**	**1.81**	**6.22**	**7.48**	**0**	**0.69**	–	**13.69**
Sd	*0.58*	*0.08*	*0.25*	*0.16*	*0.05*	*0.12*	*0.21*	*0.37*	*0.32*	*0*	*0.1*	–	–
JO244-17	60.26	0.38	18.8	3.33	0.07	0.96	2.66	3.34	9.92	0	0.3	100.02	13.26
JO244-20	60.38	0.28	19.14	3.24	0	0.69	2.6	3.15	10.22	0	0.3	100	13.37
Mean	**60.32**	**0.33**	**18.97**	**3.29**	**0.04**	**0.83**	**2.63**	**3.25**	**10.07**	**0**	**0.3**	–	**13.66**
Sd	*0.08*	*0.07*	*0.24*	*0.06*	*0.05*	*0.19*	*0.04*	*0.13*	*0.21*	*0*	*0*	–	–

JO188	SiO_2	TiO_2	Al_2O_3	FeO_{tot}	MnO	MgO	CaO	Na_2O	K_2O	P_2O_5	ClO	Total	Total Alkali
JO188-1	61.22	0.42	18.77	3.18	0.11	0.67	2.26	3.62	9.39	0	0.36	100	13.01
JO188-2	60.43	0.52	18.89	3.4	0.09	0.77	2.63	3.44	9.48	0	0.35	100	12.92
JO188-3	60.11	0.49	18.71	3.74	0.12	0.93	2.87	3.13	9.59	0	0.31	100	12.72
JO188-4	61.3	0.33	18.7	3.31	0.06	0.69	2.49	2.96	9.82	0	0.33	99.99	12.78
JO188-5	60.25	0.5	18.85	3.27	0.28	0.64	2.03	4.32	9.35	0	0.51	100	13.67
JO188-6	61.88	0.31	18.53	2.9	0.12	0.47	2.22	3.83	9.26	0	0.49	100.01	13.09
JO188-7	59.89	0.53	18.75	3.64	0.1	0.87	2.63	2.95	10.3	0	0.35	100.01	13.25
JO188-8	61.4	0.35	18.68	3.07	0.17	0.42	2.16	4.38	8.79	0	0.59	100.01	13.17
JO188-9	61.47	0.32	18.7	3.09	0	0.72	2.32	3.53	9.42	0	0.44	100.01	12.95
JO188-10	61.94	0.26	18.81	2.98	0.06	0.64	2.19	3.77	8.9	0	0.44	99.99	12.67
Mean	**60.99**	**0.4**	**18.74**	**3.26**	**0.11**	**0.68**	**2.38**	**3.59**	**9.43**	**0**	**0.42**	–	**13.02**
Sd	*0.75*	*0.1*	*0.1*	*0.27*	*0.07*	*0.16*	*0.26*	*0.5*	*0.43*	*0*	*0.09*	–	–
JO42	SiO_2	TiO_2	Al_2O_3	FeO_{tot}	MnO	MgO	CaO	Na_2O	K_2O	P_2O_5	ClO	Total	Total Alkali
JO42-1	52.98	1.79	17.85	8.38	0.25	3.27	6.79	5.3	2.68	0.38	0.33	100	7.98
JO42-2	54.6	1.63	18.1	7.39	0.22	2.39	6.14	5.65	3.03	0.51	0.31	99.97	8.68
JO42-3	53.79	1.67	17.76	8.52	0	2.72	5.9	5.57	3.23	0.51	0.32	99.99	8.8
JO42-4	54.69	1.86	18	7.45	0.28	2.03	5.45	5.72	3.67	0.54	0.3	99.99	9.39
JO42-5	53.96	1.7	17.41	7.92	0.14	2.99	6.05	5.94	3.15	0.44	0.31	100.01	9.09
JO42-7	52.51	2.23	16.55	9.77	0.25	2.84	5.86	5.18	3.94	0.54	0.33	100	9.12
JO42-8	53.88	1.83	17.81	8.41	0.09	2.57	5.24	5.97	3.56	0.38	0.26	100	9.53
JO42-9	61.35	0.53	18.75	3.06	0.24	0.54	2.18	3.96	8.9	0	0.49	100	12.86
JO42-11	54.2	1.84	17.05	8.13	0.24	2.98	6.23	5.23	3.32	0.51	0.27	100	8.55
JO42-12	56.22	1.5	19.13	5.45	0.09	1.12	5.24	6.53	3.93	0.44	0.34	99.99	10.46
JO42-13	54.61	1.86	17.53	7.68	0.18	2.38	5.28	5.67	3.89	0.57	0.35	100	9.56
Mean	**54.8**	**1.68**	**17.81**	**7.47**	**0.18**	**2.35**	**5.49**	**5.52**	**3.94**	**0.44**	**0.33**	–	**9.46**
Sd	*2.38*	*0.42*	*0.72*	*1.8*	*0.09*	*0.83*	*1.2*	*0.65*	*1.7*	*0.16*	*0.06*	–	–

Sea cores (Keller et al., 1978), and successively in a Tyrrhenian Sea core (Paterne et al., 2008) and in the Lago Grande di Monticchio succession (Wulf et al., 2007). This is the first recognition of X6 tephra layer in the Balkans, and it considerably enlarges its dispersal area to the east (Fig. 5b).

5.1.3. Tephra layer JO-244

This tephra layer is 11 cm thick (Fig. 2) and comprises both glass shards and micropumice fragments. When plotted on TAS diagram, the glass composition has a narrow variability within the trachytic and phonolitic fields (Fig. 3d). However, the tephra layer shows a variable alkali ratio passing from the base to the top. In particular, the basal part shows the coexistence of glasses with two different alkali ratios (Table 2), whereas the upper part has a very homogeneous LAR-trachytic glass composition (Table 2).

The glass composition indicates the Campanian area as the source for this tephra that, on the basis of the peculiar variability in alkali ratio and the deposit thickness, can be confidently correlated to the Campanian Ignimbrite eruption from Campi Flegrei. The geochemical comparison of major elements shown in Table 3 is applied with the ML-2 layer (Margari et al., 2007) and the TM-18 layer (Wulf et al., 2004) among the many analyses available. The Campanian Ignimbrite eruption was dated at 39,280 ± 110 years ($^{40}Ar/^{39}Ar$ technique; (De Vivo et al., 2001)), and corresponds to the Y5 tephra layer, widely dispersed in the central and eastern Mediterranean and in mainland Europe (Giacco et al., 2008; Keller et al., 1978; Margari et al., 2007; Narcisi and Vezzoli, 1999; Paterne et al., 1986; Paterne et al., 1988; Pyle et al., 2006; Sulpizio et al., 2003; Vezzoli, 1991; Wagner et al., 2008b; Wulf et al., 2004). The recognition in Albanian side of Lake Ohrid succession confirms the previous finding of Wagner et al. (2008b) from the Macedonian side of the lake (Fig. 5c).

5.1.4. Tephra layer JO-187

The JO-187 tephra is chronogically constrained between the Campanian Ignimbrite (≈39 ka) and the ^{14}C age of 9,407 ± 121 cal yr BP obtained at 100 cm depth (Table 1; Fig. 2a). The homogeneous trachytic composition (Table 2, Fig. 3e) of this tephra layer suggests it originated from the Campanian volcanic zone, and shows a good match with the composition of SMP1-e eruption from Campi Flegrei (Di Vito et al., 2008). The SMP1-e eruption corresponds to the Y3 tephra layer (Table 3; Di Vito et al., 2008; Sulpizio et al., 2003; Zanchetta et al., 2008), which is widely dispersed in the central Mediterranean area (Keller et al., 1978; Munno and Petrosino, 2006; Narcisi and Vezzoli, 1999; Sulpizio et al., 2003; Wulf et al., 2004; Zanchetta et al., 2008) with an estimated age between 30 and 31 cal ka BP (Zanchetta et al., 2008). The recognition in Albanian side of Lake Ohrid succession confirms the previous finding of Wagner et al. (2008b) from the Macedonian side of the lake (Fig. 5d).

5.1.5. Cryptotephra JO-42

This cryptotephra is stratigraphically younger than the ^{14}C age of 6,680 ± 66 cal yr BP (Table 1), and the mugearitic-benmoreitic composition easily indicates the Mount Etna as the source. The shallow position within the core and the glass composition indicates a correlation with the FL eruption from Mount Etna, dated at 3,370 ± 70 cal yr BP (Coltelli et al., 2000; Wagner et al., 2008b). The recognition in Lake Ohrid succession confirms the previous finding in the same lake (Macedonian side) (Wagner et al., 2008b) and in the Lake Shkodra successions (Albania) (Fig. 5e; (Sulpizio et al., 2010)).

Table 3
Comparison of the composition of the recognised tephra layers with analyses from literature: KET 8222 340 cm, 350 cm, 555 cm, 563 cm, 765 cm, DED 8708 1209 cm from Paterne (1985) and Paterne et al. (2008); ML-2 from Margari et al. (2007); TM-15 and TM-18 from Wulf et al. (2004); MD90-917 920 cm from Zanchetta et al. (2008); tephra Ohrid 310-315 cm from Wagner et al. (2008b); Pergusa type A and B from Sadori and Narcisi (2001) and PRG06-03 390 cm and SK13 514 cm from Sulpizio et al. (2010).

Tableau 3
Comparaison des moyennes et des écarts-types des compositions des niveaux de tephra identifiés aux analyses issues de la littérature : KET 8222 340 cm, 350 cm, 555 cm, 563 cm, 765 cm, DED 8708 1209 cm d'après Paterne (1985) et Paterne et al. (2008) ; ML-2 d'après Margari et al. (2007) ; TM-15 et TM-18 d'après Wulf et al. (2004) ; MD90-917 920 cm d'après Zanchetta et al. (2008) ; tephra Ohrid 310-315 cm d'après Wagner et al. (2008b) ; Pergusa type A et B d'après Sadori and Narcisi (2001) et PRG06-03 390 cm et SK13 514 cm d'après Sulpizio et al. (2010).

		SiO_2	TiO_2	Al_2O_3	FeO_{tot}	MnO	MgO	CaO	Na_2O	K_2O	P_2O_5	SO_3	ClO	F	Total Alkali
KET 8222 563 cm	Mean	73.09	0.39	8.88	7.05	–	0.09	0.27	5.81	4.42	–	–	–	–	10.23
n = 13	*sd*	*0.36*	*0.08*	*0.13*	*0.12*	–	*0.06*	*0.11*	*0.37*	*0.16*	–	–	–	–	–
KET 8222 555 cm	Mean	72.95	0.31	8.89	7.23	–	0.05	0.20	5.90	4.48	–	–	–	–	10.38
n = 13	*sd*	*0.47*	*0.05*	*0.05*	*0.33*	–	*0.03*	*0.04*	*0.36*	*0.10*	–	–	–	–	–
KET 8222 765 cm	Mean	72.97	0.50	9.02	7.34	–	0.10	0.20	5.44	4.42	–	–	–	–	9.86
	sd	*0.49*	*0.06*	*0.16*	*0.28*	–	*0.07*	*0.02*	*0.30*	*0.06*	–	–	–	–	–

		SiO_2	TiO_2	Al_2O_3	FeO_{tot}	MnO	MgO	CaO	Na_2O	K_2O	P_2O_5	SO_3	ClO	F	Total Alkali
KET8222 350 cm	Mean	61.47	0.52	19.20	3.20	–	0.40	1.66	6.27	7.30	–	–	–	–	13.56
n = 11	*sd*	*0.06*	*0.04*	*0.10*	*0.22*	–	*0.06*	*0.10*	*0.53*	*0.77*	–	–	–	–	
KET8222 340 cm	Mean	61.98	0.47	19.18	3.06	–	0.42	1.70	6.08	7.11	–	–	–	–	13.19
n = 14	*sd*	*0.27*	*0.10*	*0.13*	*0.15*	–	*0.09*	*0.10*	*0.68*	*0.46*	–	–	–	–	
DED 8708 1209 cm	Mean	61.81	0.48	18.18	3.04	0.33	0.31	1.71	5.72	7.29	0.02	0.11	0.97	–	13.02
n = 19	*sd*	*0.68*	*0.10*	*0.31*	*0.23*	*0.12*	*0.07*	*0.32*	*0.91*	*0.86*	*0.04*	*0.08*	*0.28*	–	–

		SiO_2	TiO_2	Al_2O_3	FeO_{tot}	MnO	MgO	CaO	Na_2O	K_2O	P_2O_5	SO_3	ClO	F	Total Alkali
TM-18	Mean	61.69	0.42	19.11	2.93	0.24	0.35	1.73	5.66	6.83	0.05	–	0.78	0.19	12.49
n = 43	*sd*	*0.46*	*0.02*	*0.21*	*0.09*	*0.02*	*0.02*	*0.07*	*0.71*	*0.29*	*0.03*	–	*0.05*	*0.17*	–
ML-2	Mean	61.01	0.48	18.18	3.02	0.21	0.44	2.12	5.64	8.05	0.07	–	0.71	–	13.7
n = 105	*sd*	*0.42*	*0.04*	*0.19*	*0.21*	*0.06*	*0.15*	*0.32*	*1.21*	*1.02*	*0.04*	–	*0.20*	–	–

		SiO_2	TiO_2	Al_2O_3	FeO_{tot}	MnO	MgO	CaO	Na_2O	K_2O	P_2O_5	–	ClO	F	Total Alkali
TM-15	Mean	62.22	0.38	18.36	3.27	0.13	0.61	2.19	3.85	8.36	0.12	–	0.52	0	12.21
n = 20	*sd*	*0.78*	*0.03*	*0.21*	*0.29*	*0.04*	*0.15*	*0.22*	*0.44*	*0.55*	*0.06*	–	*0.11*	*0*	–
MD90-917 920 cm	Mean	61.41	0.36	18.72	3.17	0.08	0.70	2.44	3.52	9.14	–	–	0.44	–	12.66
n = 20	*sd*	*0.86*	*0.12*	*0.17*	*0.38*	*0.08*	*0.21*	*0.33*	*0.40*	*0.40*	–	–	*0.09*	–	–

		SiO_2	TiO_2	Al_2O_3	FeO_{tot}	MnO	MgO	CaO	Na_2O	K_2O	P_2O_5	SO_3	ClO	F	Total Alkali
SK13 514 cm	Mean	56.81	1.21	20.52	4.86	0.09	1.38	5.27	6.22	3.10	0.24	–	0.30	–	9.32
n = 14	*sd*	*1.78*	*0.44*	*2.39*	*2.49*	*0.09*	*1.27*	*1.83*	*1.04*	*1.26*	*0.22*	–	*0.11*	–	–
Tephra Ohrid 310–315 cm	Mean	54.25	1.76	17.48	8.15	0.00	2.85	6.02	5.40	3.29	0.48	–	0.31	–	8.69
n = 15	*sd*	*0.73*	*0.22*	*0.51*	*0.53*	*0.00*	*0.33*	*0.50*	*0.41*	*0.34*	*0.10*	–	*0.06*	–	–
PRG06-03 390 cm	Mean	52.82	2.04	16.86	9.43	0.23	3.21	6.13	4.99	3.58	0.47	–	0.24	–	8.57
n = 11	*sd*	*0.82*	*0.17*	*0.47*	*0.90*	*0.10*	*0.42*	*1.03*	*0.37*	*0.67*	*0.07*	–	*0.06*	–	–
Type A Pergusa	Mean	55.61	1.58	16.97	7.25	0.15	3.98	5.62	6.02	2.37	–	–	0.46	–	8.39
n = 14	*sd*	*2.28*	*0.20*	*0.78*	*1.35*	*0.09*	*0.57*	*0.95*	*1.13*	*0.34*	–	–	*0.09*	–	–
Type B Pergusa	Mean	54.91	1.61	17.65	6.83	0.15	3.90	5.65	5.79	3.06	–	–	0.45	–	8.86
n = 11	*sd*	*0.91*	*0.23*	*0.49*	*1.16*	*0.09*	*0.47*	*1.04*	*0.88*	*0.25*	–	–	*0.43*	–	–

5.2. Significance of tephra layer recognition in Lake Ohrid

The recognition of tephra layers in the Lake Ohrid has relevance for both volcanology and Quaternary Sciences.

From a volcanological point of view, the five tephra layers recognised in the sediments testify for episodes of ash deposition in very distal areas with respect to the Italian volcanoes (Fig. 5), irrespective if they are from large (P11, X6, Y5 and Y3 tephra layers) or intermediate (FL tephra layer) explosive eruptions.

Three out of five tephra layers were already recognised in Lake Ohrid sediments (Y5, Y3, and FL), but from a core located in the Macedonian side of the lake (Wagner et al., 2008b). Their recognition in core JO 2004, confirms their deposition was not sporadic but probably they affected all the lake area and its drainage basin. Two of them (P11 and X6) were recognised for the first time in the Balkan area, significantly enlarging to the northeast their dispersal that was previously limited to Ionian and Tyrrhenian seas (Keller et al., 1978; Paterne et al., 2008) or Lago Grande di Monticchio (Wulf et al., 2007).

The distance between the studied site and the inferred source areas is 550 km for the Campanian volcanic area, 620 km for Mount Etna and 900 km for Pantelleria Island (Fig. 5). Bearing in mind that they represent minimum values, the area affected by ash deposition can be assessed at ca. 207,000 km^2 for P11, ca. 471,000 km^2 for X6, at ca. 550,000 km^2 for the Y3 tephra layers. The dispersal area of the Y5 was previously assessed between $1.5–3 \times 10^6$ km^2 (Pyle et al., 2006).

The paucity of accurate studies on distal ash deposits mainly relies in their poor preservation and in their

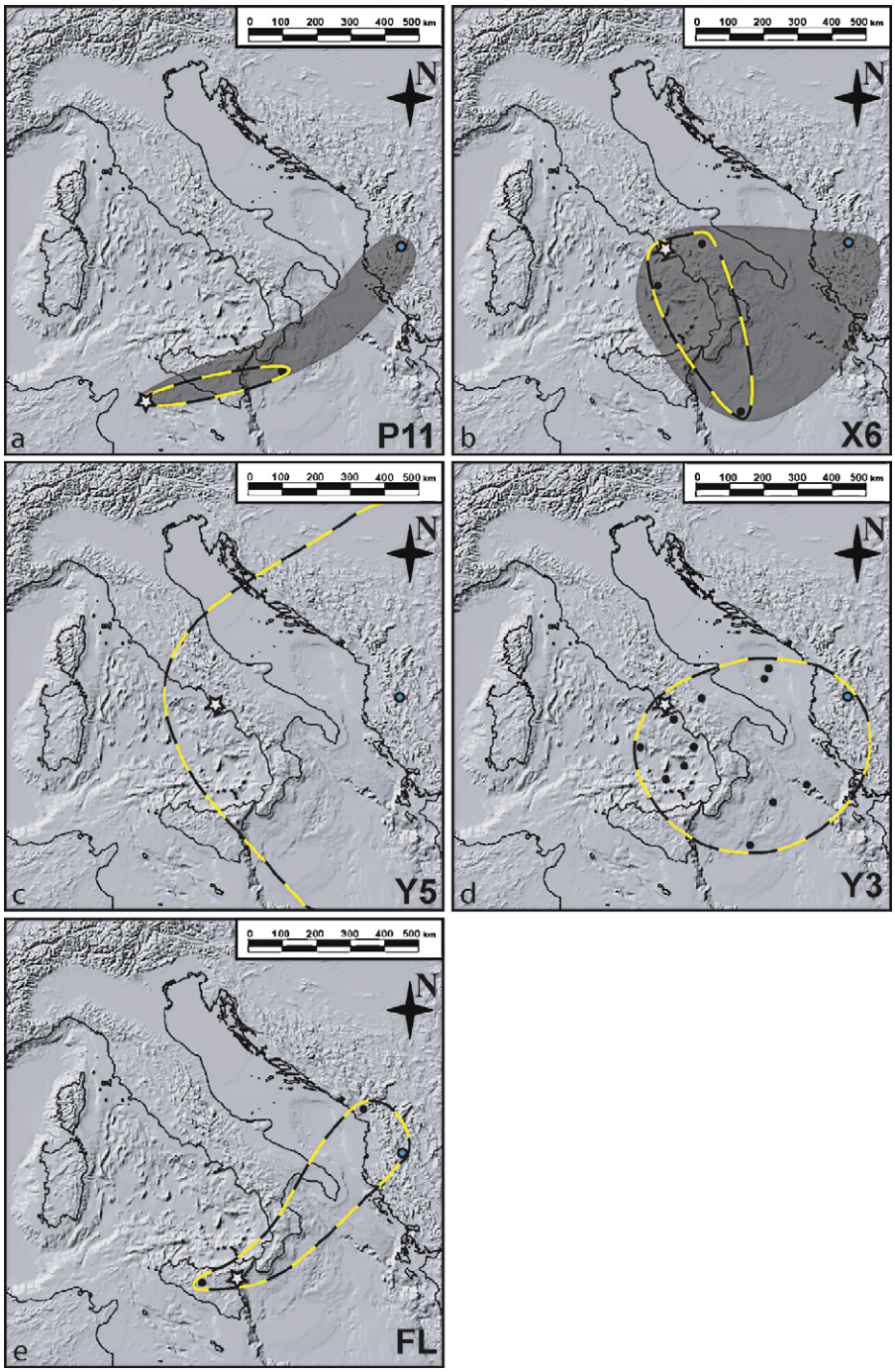

Fig. 5. Reconstructed dispersal areas of the five tephra layers recognised in core JO 2004 and using previously published data. (a) P11 tephra layer. The dashed line indicates the previous inferred dispersal area. KET 8222, data from Paterne et al. (2008); (b) X6 tephra layer. The dashed line indicates the previous inferred dispersal area. KET 8222 and DED 8708 data from Paterne et al. (2008); (c) Y5 tephra layer. Dispersal area from (Giacco et al., 2008; Pyle et al., 2006); (d) Y3 tephra layer. C6 and C145 data from Munno and Petrosino (2004), V10-68, RC9-190, 22M60 data from Keller et al. (1978), KET 8004 and KET 8011 data from Paterne et al. (2008) and Zanchetta et al. (2008), LZ 1120 data from Wagner et al. (2008b) and MD90-917 data from Paterne et al. (1986) and Zanchetta et al. (2008); (e) FL dispersal area is from Sulpizio et al. (2010). Blue dots indicate the location of the JO 2004 core. Stars indicate the volcanic sources.

Fig. 5. Reconstruction des zones de dispersion des cinq éruptions identifiées dans la carotte JO 2004 : (a) les tephra de P11 ont été identifiés dans la carotte KET 8222 (Paterne et al., 2008) ; (b) les tephra de X6 ont été identifiés dans les carottes KET 8222 et DED 8708 (Paterne et al., 2008) ; (c) la carte de dispersion des cendres de Y5 est modifiée à partir de Giacco et al. (2008) ; Pyle et al. (2006) ; (d) les tephra de Y3 ont été identifiés dans les carottes C6 et C145 (Munno et Petrosino, 2004), V10-68, RC9-190, 22M60 (Keller et al., 1978), KET 8004 et KET 8011 (Paterne et al., 2008 ; Zanchetta et al., 2008), LZ 1120 (Wagner et al., 2008b) et MD90-917 (Paterne et al., 1986 ; Zanchetta et al., 2008) ; (e) la carte de dispersion des cendres de Etna FL est modifiée à partir de Sulpizio et al. (2010). Les points bleus indiquent la localisation de la carotte JO 2004. Les étoiles indiquent les sources volcaniques et les précédentes surfaces de dispersion sont limitées par un trait jaune et noir.

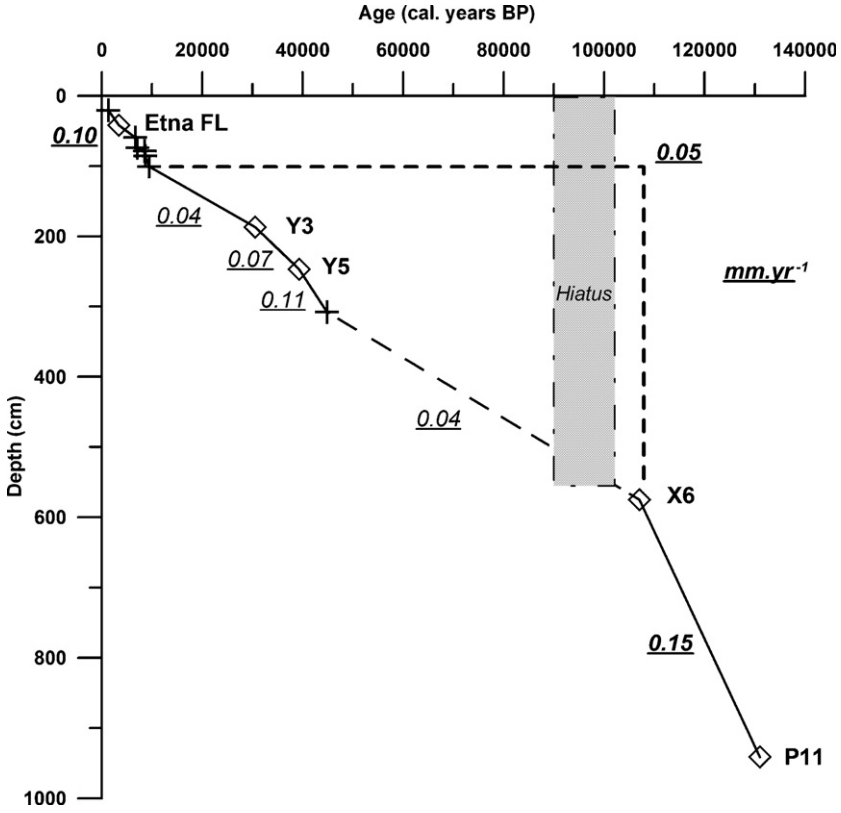

Fig. 6. Sedimentation curves for core JO 2004 calculated using the available calibrated ^{14}C (cross) and the correlated ages of tephra layers (diamonds). The grey-shaded area indicates the inferred sedimentary hiatus. P11 = JO-941, X6 = JO-575, Y5 = JO-245, Y3 = JO-187, Etna FL = JO-42. Numbers in italic underlined indicate the calculated sedimentation rate ($mm.yr^{-1}$) for each segment of the curve.

Fig. 6. Courbe de sédimentation de la carotte JO 2004 calculée à partir des âges ^{14}C calibrés (croix) et des datations corrélées aux niveaux de tephra (losanges). La zone grisée indique le hiatus sédimentaire. P11 = JO-941, X6 = JO-575, Y5 = JO-245, Y3 = JO-187, Etna FL = JO-42. Les chiffres soulignés en italiques représentent le taux de sédimentation ($mm.an^{-1}$) pour chaque section de la courbe.

dispersal behaviour. The accumulation of volcanic ash in distal zones often represents a hazard, since most of the attention and mitigation procedures are usually devoted to proximal areas. Deposition of ash in distal sites can cause damage to infrastructures, disturbance to communications, water pollution and breathing problems. Therefore the recognition and the collection of very distal samples can improve hazard mitigation plans and procedures over very large area far from the volcanic sources.

From a Quaternary Science point of view, Lake Ohrid represents an exceptional natural archive. A previous work (Wagner et al., 2008b) studied a core (Lz1120) from the Macedonian side of the lake, but analysed and discussed only the last 40 ka of sedimentation record of Lake Ohrid with a similar core length than the JO 2004. This apparent difference in sedimentation rate relies in both the presence of sedimentary hiatus in core JO 2004 (Fig. 6; (Belmecheri et al., 2009; Lézine et al., 2010)) and the different locations of the two cores, with the Lz1120 closer to the major karstic springs than the JO 2004 (Belmecheri et al., 2009).

The core JO 2004 offers the opportunity to study about 130 ky of the sedimentary record, which encompasses the last interglacial. In this scenario, the presence of two important regional markers like the P11 and X6 tephra layers allow the physical correlation of the deep part of the cores JO 2004 to other important archives of the central Mediterranean area.

The available ^{14}C datings (Table 1) and the tephra layers allow the drawing of a sedimentation curve (Fig. 6). The sedimentation curve was built using the seven ^{14}C datings and the tephrochronology, and shows three main rates of sedimentation. The first one between 0 and 100 cm is about 0.10 $mm.yr^{-1}$, the second one, between 100 and 575 cm is around 0.05 $mm.yr^{-1}$ and the third one between 575 and 988 cm is about 0.15 $mm.yr^{-1}$ (Fig. 6).

These variable sedimentation rates reflect different paleo-environmental information. Below the X6 tephra layer, there is the transition between the last-glacial and the last-interglacial phases (Eemian, transition from marine isotopic stage 5 and 6, around 125 ka BP; (Lézine et al., 2010)), which was characterised by a high sedimentation rate (0.15 $mm.yr^{-1}$; Fig. 6). Between 100 and 575 cm depth, there is a glacial period record with a low sedimentation rate (0.05 $mm.yr^{-1}$) and low sediment dynamic. It is important to note that this sedimentation rate is probably underestimated, since it does not take into account the occurrence of the inferred sedimentary hiatus between 90 and 103 ka (Fig. 6; (Belmecheri et al., 2009)).

The upper 100 cm of core sediments (younger than 10 cal ky BP) correspond to the current interglacial period, which is characterised by a higher sedimentation rate (0.10 mm.yr^{-1}; Fig. 6).

6. Conclusions

The study of the JO 2004 cores yields some important results for the tephostratigraphy and tephrochronology of the Balkans. Five tephra layers were recognised and described, and two of them were for the first time discovered in the area. The tephra layer P11 is the oldest in the whole recognised succession and testifies for ash deposition at more than 900 km from its source on Pantelleria Island. Similarly, the recognition of tephra layer X6 enlarges to the east its dispersal, since it was previously described only in Ionian and Tyrrhenian Sea cores and in the Lago Grande di Monticchio. The other three tephra layers (FL, Y3 and Y5) were already recognised in Lake Ohrid succession, and the new findings testify for their extensive deposition in the area.

The recognition of the two deeper tephra layers (X6 and P11) is especially important, since they allow the establishment of a chronology for the part of the core older than 40 ka BP, and its physical link to other archives of the central Mediterranean area.

In perspective, this work will allow one to obtain a better estimation of the distal tephra dispersion from Italian volcanoes. These results must be integrated in the mitigation and rescue plans that concern the population of the central Mediterranean area.

Acknowledgements

We acknowledge the French (INSU-CNRS) research program ECLIPSE, the French School of Athens (Greece) and the Archaeological museum of Korça (Albania) for financial support and authorizations. We thank Anne-Marie Lézine, Uli von Grafenstein and Nils Andersen for providing samples for the piston core JO 2004 and for the useful discussions. Alain Mazaud is thanked for the magnetic susceptibility. BC was partially supported by Vinci program of Université Franco-Italienne and SETCI from region of Île-de-France. Franco Colarieti (DST Pisa) is gratefully acknowledged for the preparation of samples and assistance during EDS analyses. Amandine Bordon, Soumaya Belmecheri and Sonia La Felice are thanked for helpful discussions. An anonymous reviewer provided helpful suggestions for improving the manuscript.

References

Aliaj, S., 2000. Neotectonics and seismicity in Albania. In: Meco, S., Aliaj, S., Turku, I. (Eds.), Geology of Albania, vol. 28. Beitrage zur regionalen Geologie der Erde, Gebrüder Bornträger, Berlin, pp. 135–178.

Aliaj, S., Baldassarre, G., Shkupi, D., 2001. Quaternary subsidence zones in Albania: some case studies. Bull. Eng. Geol. Environ. 59, 313–318.

Aliaj, S., Adams, J., Halchuk, S., Sulstarova, E., Peci, V., Muco, B., 2004. Probabilistic seismic hazard maps for Albania. In: 13th World conference earthquake engineering, Vancouver, BC, Canada, paper no. 2469, 14 p.

Anovski, T., Naumovski, J., Kacurkov, D., Kirkov, P., 1980. A study of the origin of waters of St. Naum Springs, Lake Ohrid (in Macedonian). Fisica 12, 76–86.

Bard, E., Arnold, M., Hamelin, B., Tisnerat-Laborde, N., Cabioch, G., 1998. Radiocarbon calibration by means of mass spectrometric ^{230}Th/^{234}U and ^{14}C ages of corals: an updated database including samples from Barbados, Mururoa, and Tahiti, In: Stuiver, M., and van der Plicht, J. (Eds.), INTCAL98: calibration issue. Radiocarbon 40, 1085–1092.

Belmecheri, S., Namiotko, T., Robert, C., von Grafenstein, U., Danielopold, D.L., 2009. Climate controlled ostracod preservation in Lake Ohrid next term (Albania, Macedonia). Palaeogeogr. Palaeoclimatol. Palaeoecol. 277 (3–4), 236–245.

Calanchi, N., Cattaneo, A., Dinelli, E., Gasparotto, G., Lucchini, F., 1998. Tephra layers in Late Quaternary sediments of the central, Adriatic Sea. Marine Geology 149, 191–209.

Coltelli, M., Del Carlo, P., Vezzoli, L., 2000. Stratigraphic constraints for explosive activity in the past 100 ka at Etna volcano, Italy. Int. J. Earth Sciences 89, 665–677.

De Vivo, B., Rolandi, G., Gans, P.B., Calvert, A., Bohrson, W.A., Spera, F.J., Belkin, H.E., 2001. News constraints on the pyroclastic eruptive history of the Campanian volcanic Plain (Italy). Mineralogy Petrology 73, 47–65.

Di Vito, M.A., Sulpizio, R., Zanchetta, G., D'Orazio, M., 2008. The Late Pleistocene pyroclastic deposits of the Campanian Plain: new insights into the explosive activity of Neapolitan volcanoes. J. Volcanol. Geotherm. Res. 177, 19–48 (doi:10.1016/j.jvolgeores.2007.11.019).

Giaccio, B., Isaia, R., Fedele, F.G., Di Canzio, E., Hoffecker, J., Ronchitelli, A., Sinitsyn, A., Anikovich, M., Lisitsyn, S.N., 2008. The Campanian Ignimbrite and Codola tephra layers: two temporal/stratigraphic markers for the early Upper Palaeloithic in southern Italy and eastern Europe. J. Volcanol. Geotherm. Res. 177, 208–226 (doi:10.1016/j.jvolgeores.2007.10.007).

Goldsworthy, M., Jackson, J., Haines, J., 2002. The continuity of active fault systems in Greece. Geophys. J. Int. 148, 596–618.

GSA Rock Color Chart, 1991. The Geological Society of America Rock-Color Chart with genuine Munsell color chips. Printed by Munsell Color USA.

Hadzisce, S.D., 1966. Das Mixophänomen im Ohridsee im Laufe der Jahre 1941/42-1964/65. Verh. Internat. Verein. Limnol. 16, 134–138.

Keller, J., Ryan, W.B.F., Ninkovich, D., Altherr, R., 1978. Explosive volcanic activity in the Mediterranean over the past 200,000 yr as recorded in deep-sea sediments. Geol. Soc. Am. Bull. 89, 591–604.

Kraml, M., 1997. Laser- ^{40}Ar/^{39}Ar-Datierungen an distalen marinen Tephren des jung-quartären mediterranen Vulkanismus (Ionishes Meer, METEOR-Fahrt 25/4), Ph.D. Thesis, Albert-Ludwigs-Universität Freiburg i.Br. p. 216.

La Felice, S., Rotolo, S.G., Scaillet, S., Vita, G., 2009. Tephrostratigraphy, petrochemistry and ^{40}Ar–^{39}Ar age data on Pre-Green Tuff sequences, Pantelleria, Congresso Fist Geoitalia 2009, I 7- Dal terreno al laboratorio: approcci multidisciplinari per lo studio del vulcanismo esplosivo.

Le Bas, M.J., Le Maitre, R.W., Streckeisen, A., Zanettin, B., 1986. A chemical classification of volcanic rocks based on the total alkali-silica diagram. J. Petrol. 27, 745–750.

Lézine, A.M., von Grafenstein, U., Andersen, N., Belmecheri, S., Bordon, A., Caron, B., Cazet, J.P., Erlenkeuser, H., Fouache, E., Grenier, C., Huntsman-Mapila, P., Hureau-Mazaudier, D., Manelli, D., Mazaud, A., Robert, C., Sulpizio, R., Tiercelin, J.J., Zanchetta, G., Zeqollari, Z., 2010. Lake Ohrid, Albania, provides an exceptional multi-proxy record of environmental changes during the last glacial-interglacial cycle. Palaeogeogr. Palaeoclimatol. Palaeoecol. (doi:10.1016/j.palaeo.2010.01.016).

Lowe, J.J., Blockley, S., Trincardi, F., Asioli, A., Cattaneo, A., Matthews, I.P., Pollard, M., Wulf, S., 2007. Age modelling of late Quaternary marine sequences in the Adriatic: towards improved precision and accuracy using volcanic event stratigraphy. Continental Shelf Res 27, 560–582.

Macdonald, R., 1974. Nomenclature and petrochemistry of the peralkaline oversaturated extrusive rocks. Bull. Volcanol. 38, 498–516.

Magny, M., de Beaulieu, J.L., Drescher-Schneider, R., Vannnière, B., Walter-Simmonet, A.V., Millet, L., Bossuet, G., Peyron, O., 2006. Climatic oscillations in central Italy during the Last Glacial-Holocene transition: the record from Lake Accesa. J. Quat. Sci. 21, 311–320.

Magny, M., de Beaulieu, J.L., Drescher-Schneider, R., Vanniére, B., Walter-Simonnet, A.V., Miras, Y., Millet, L., Bossuet, G., Peyron, O., Brugiapaglia, E., Leroux, A., 2007. Holocene climate changes in the central Mediterranean as recorded by lake-level fluctuations at Lake Accesa (Tuscany, Italy). Quat. Sc. Rev. 26, 1736–1758.

Mahood, G.A., Hildreth, W., 1986. Geology of the peralkaline volcano at Pantelleria, Strait of Sicily. Bull. Volcanol. 48, 143–172.

Margari, V., Pyle, D.M., Bryant, C., Gibbard, P.L., 2007. Mediterranean tephra stratigraphy revisited: Results from a long terrestrial sequence on Lesvos Island, Greece. J. Volcanol. Geotherm. Res. 163, 34–54.

Marianelli, P., Sbrana, A., 1998. Risultati di misure di standard di minerali e di vetri naturali in microanalisi a dispersione di energia. Atti Societa Toscana di Scienze Naturali Memorie Serie A 105, 57–63.

Matzinger, A., Jordanoski, M., Veljanoska-Sarafiloska, E., Sturm, M., Müller, B., Wüest, A., 2006. Is Lake Prespa jeopardizing the ecosystem of ancient Lake Ohrid? Hydrobiologica 553, 89–109.

Munno, R., Petrosino, P., 2004. New constraints on the occurrence of Y3 Upper Pleistocene tephra marker layer in the Tyrrhenian Sea. Italian J. Quat. Sci. 17 (1), 11–20.

Munno, R., Petrosino, P., 2006. The Late Quaternary tephrostratigraphical record of the San Gregorio Magno basin (southern Italy). J. Quat. Sci. 22, 247–266 (doi:10.1002/jqs.1025).

Narcisi, B., Vezzoli, L., 1999. Quaternary stratigraphy of distal tephra layers in the Mediterranean – an overview. Global Planetary Change 21, 31–50.

Nicot, J., Chardon, M., 1983. On the morphotectonic background and the evolution of natural environments and limestone relief in Western Yugoslavian Macedoni. Mediterranee 37–52.

Pappalardo, L., Civetta, L., D'Antonio, M., Deino, A., Di Vito, M.A., Orsi, G., Carandente, A., de Vita, S., Isaia, R., Piochi, M., 1999. Chemical and Sr-isotopical evolution of the Phlegraen magmatic system before the Campanian Ignimbrite and the Neapolitan Yellow Tuff eruptions. J. Volcanol. Geotherm. Res. 91, 141–166.

Paterne, M., 1985. Reconstruction de l'activité explosive des volcans de l'Italie du Sud par téphrochronologie marine, Ph.D. Thesis University of Paris Sud XI, Paris. 144 p.

Paterne, M., Guichard, F., Labeyrie, J., Gillot, P.Y., Duplessy, J.C., 1986. Tyrrhenian Sea tephrochronology of the oxygen isotope record for the past 60,000 years. Marine Geology 72, 259–285.

Paterne, M., Guichard, F., Labeyrie, J., 1988. Explosive activity of the South Italian volcanoes during the past 80,000 years as determined by marine tephrochronology. J. Volcanol. Geotherm. Res. 34, 153–172.

Paterne, M., Labeyrie, J., Guichard, F., Massaud, A., Maitre, F., 1990. Fluctuation of the Campanian explosive activity (South Italy) during the last 190,000 years as determined by marine tephrochronology. Earth Planet. Sci. Lett. 98, 166–174.

Paterne, M., Guichard, F., Duplessy, J.C., Siani, G., Sulpizio, R., Labeyrie, J., 2008. A 90,000–200,000 yrs marine tephra record of Italian volcanic activity in the central Mediterranean Sea. J. Volcanol. Geotherm. Res. 177, 187–196 (doi:10.1016/j.jvolgeores.2007.11.028).

Poli, S., Chiesa, S., Gillot, P.Y., Guichard, F., 1987. Chemistry versus time in the volcanic complex of Ischia (Gulf of Naples, Italy): evidence of successive magmatic cycles. Contrib. Min. Petrol. 95, 322–335.

Pyle, D.M., Ricketts, G.D., Margari, V., van Andel, T.H., Sinitsyn, A.A., Praslov, N., Lisitsyn, S., 2006. Wide dispersal and deposition of distal tephra during the Pleistocene "Campanian Ignimbrite/Y5" eruption, Italy. Quat. Sci. Rev. 25, 2713–2728.

Reimer, P.J., Baillie, M.G.L., Bard, E., Bayliss, A., Beck, J.W., Bertrand, C., Blackwell, P.G., Buck, C.E., Burr, G., Cutler, K.B., Damon, P.E., Edwards, R.L., Fairbanks, R.G., Friedrich, M., Guilderson, T.P., Hughen, K.A., Kromer, B., McCormac, F.G., Manning, S., Bronk Ramsey, C., Reimer, R.W., Remmele, S., Southon, J.R., Stuiver, M., Talamo, S., Taylor, F.W., van der Plicht, J., Weyhenmeyer, C.E., 2004. InterCal04 terrestrial radiocarbon age calibration, 0–26 kyrBP. Radiocarbon 46, 1029–1058.

Sadori, L., Narcisi, B., 2001. The Postglacial record of environmental history from Lago di Pergusa, Sicily, The Holocene 11 (6), 655–670 (doi:10.1191/09596830195681).

Santacroce, R. (Ed.), 1987. Somma-Vesuvius, CNR Quaderni Ricerca Scientifica 114, 251.

Santacroce, R., Cioni, R., Marianelli, P., Sbrana, A., Sulpizio, R., Zanchetta, G., Donahue, D.J., Joron, J.L., 2008. Age and whole rock-glass compositions of proximal pyroclastics from the major explosive eruptions of Somma-Vesuvius: a review as a tool for distal tephrostratigraphy, J. Volcanol. Geotherm. Res. 177, 1–18 (doi:10.1016/j.jvolgeores.2008.06.009).

Siani, G., Sulpizio, R., Paterne, M., Sbrana, A., 2004. Tephrostratigraphy study for the last 18,000 ^{14}C years in a deep-sea sediment sequence for the South Adriatic. Quat. Sci. Rev. 23, 2485–2500.

Stankovic, S., 1960. The Balkan Lake Ohrid and its living world, Monographiae Biologicae IX, Dr. W. Junk, Den Haag, 357.

Stankovic, S., Hadzisce, S.D., 1953. La thermique du lac d'Ohrid. Recueil des traveaux. Station hydrobiologique – Ohrid 61.

Sulpizio, R., Zanchetta, G., Paterne, M., Siani, G., 2003. A review of tephrostratigraphy in central and southern Italy during the last 65 ka. Il Quaternario 16, 91–108.

Sulpizio, R., Bonasia, R., Dellino, P., Di Vito, M.A., La Volpe, L., Mele, D., Zanchetta, G., Sadori, L., 2008. Discriminating the long distance dispersal of fine ash from sustained columns or near ground ash clouds: the example of the Pomici di Avellino eruption (Somma-Vesuvius, Italy), J. Volcanol. Geotherm. Res. 177, 263–276 (doi:10.1016/j.jvolgeores.2007.11.012).

Sulpizio, R., van Welden, A., Caron, B., Zanchetta, G., 2010. The Holocene tephrostratigraphic record of Lake Shkodra (Albania and Montenegro), J. Quat. Sci. (doi:10.1002/jqs.1334).

Thunnell, R., Federman, A., Sparks, S., Williams, D., 1978. The age, origin and volcanological significance of the Y-5 ash layer in the Mediterranean. Quaternary Res. 12, 241–253.

Tzedakis, P.C., Frogley, M.R., Heaton, T.H.E., 2003. Last interglacial conditions in southern Europe: evidence from Ioannina, northwest Greece, Global and Planetary Change 36, 157–170 (doi:10.1016/S0921-8181(02)00182-0).

Vezzoli, L., 1988. Island of Ischia. CNR, Quaderni della Ricerca Scientifica 114, 230.

Vezzoli, L, 1991. Tephra layers in Bannock Basin (Eastern Mediterranean). Mar. Geol. 100, 21–34.

Wagner, B., Reicherter, K., Daut, G., Wessels, M., Matzinger, A., Schwalb, A., Spirkovski, Z., Sanxhaku, M., 2008a. The potential of Lake Ohrid for long-term palaeoenvironmental reconstructions, Palaeogeogr., Palaeoclimatol., Palaeoecol. 259, 341–356 (doi:10.1016/j.palaeo.2007.10.015).

Wagner, B., Sulpizio, R., Zanchetta, G., Wulf, S., Wessels, M., Daut, G., Nowaczyk, N., 2008b. The last 40 ka tephrostratigraphic record of Lake Ohrid, Albania and Macedonia: a very distal archive for ash dispersal from Italian volcanoes, J. Volcanol. Geotherm. Res. 177, 71–80 (doi:10.1016/j.jvolgeores.2007.08.018).

Wulf, S., Kraml, M., Brauer, A., Keller, J., Negendank, J.F.W., 2004. Tephrochronology of the 100 ka lacustrine sediment record of Lago Grande di Monticchio (southern Italy). Quaternary International 122, 7–30.

Wulf, S., Brauer, A., Mingram, J., Zolitschka, B., Negendank, J.F.W., 2007. Distal tephras in the sediments of Monticchio maar lakes, In: C. Principe, Editor, La Geologia del Monte Vulture, Regione Basilicata – Consiglio Nazionale delle Ricerche, pp. 105–122.

Zanchetta, G., Sulpizio, R., Giaccio, B., Siani, G., Paterne, M., Wulf, S., D'Orazio, M., 2008. The Y-3 tephra: a last glacial stratigraphic marker for the central Mediterranean basin. J. Volcanol. Geotherm. Res. 177, 145–154 (doi:10.1016/j.jvolgeores.2007.08.017).